3 Biotech (2022) 12:42
https://doi.org/10.1007/s13205-021-03107-w

SHORT REPORTS

Modification of thermally expanded graphite and its effect on the properties of the amperometric biosensor

Yulia Plekhanova[1] · Sergei Tarasov[1] · Anna Kitova[1] · Vladimir Kolesov[2] · Vadim Kashin[2] · Ashok K. Sundramoorthy[3] · Anatoly Reshetilov[1]

Received: 25 October 2021 / Accepted: 29 December 2021 / Published online: 15 January 2022
© King Abdulaziz City for Science and Technology 2022

Abstract

The work considered the properties of a biosensor based on a novel nanomaterial—modified thermally expanded graphite (TEG_M). The main focus was on whether the procedure of additional graphite thermal expansion would affect the electrochemical properties of biosensors based on membrane fractions of acetic acid bacteria *Gluconobacter oxydans*. Raman spectroscopy, scanning electron microscopy and electrochemical analysis were used for the study. Raman spectra showed that the formation of TEG_M led to its stratification into smaller particles and a better orderly layered structure with high "graphenization" degree. Modification of TEG led to the formation of additional cavities into which bacterial cells or bacterial membrane fractions could be immobilized and affect the electrical conductivity of the biosensors positively. Calculation of the heterogeneous charge transfer constants showed that processes occurring on the electrodes are quasi-reversible. The limiting stage of these processes is the transfer of an electron from a biological component on the electrode surface, not the diffusion of the analyte from the solution to the active centers of the enzyme. We showed the possibility of developing third-generation mediator-free biosensors for glucose detection based on TEG_M, as well as of second-generation mediator biosensors for glucose, ethanol and glycerol detection.

Keywords Thermally expanded graphite · Biosensor · Carbon nanomaterials · Electrochemical properties · *Gluconobacter oxydans*

Introduction

The application of microbial electrochemical technologies as biosensors and microbial fuel cells (MFCs) has attracted considerable research interest in recent years (Do et al. 2019; Sun et al. 2019; Li et al. 2020). These devices are based on electroactive biofilms, which are able to transfer electrons derived from the metabolic oxidation of organic substrates to the electrode. To expand the field of application of these bioelectrochemical systems, the researchers focused on screening electrochemically active model microorganisms (Guo et al. 2020), selecting conditions for their immobilization (Berillo et al. 2021), and selecting and optimizing nanomaterials to be incorporated into the electrodes (Hwang

✉ Yulia Plekhanova
plekhanova@ibpm.pushchino.ru

Sergei Tarasov
setar25@gmail.com

Anna Kitova
kitova@ibpm.pushchino.ru

Vladimir Kolesov
kvv@cplire.ru

Vadim Kashin
vadim_kashin@mail.ru

Ashok K. Sundramoorthy
ashokkumar.sun@ktr.srmuniv.ac.in

Anatoly Reshetilov
anatol@ibpm.pushchino.ru

[1] G.K. Skryabin Institute of Biochemistry and Physiology of Microorganisms, Pushchino Centre for Biological Research, Russian Academy of Sciences, 142290 Pushchino, Russian Federation

[2] FSBIS V.A. Kotelnikov Institute of Radio Engineering and Electronics, Russian Academy of Sciences, 125009 Moscow, Russian Federation

[3] Department of Chemistry, SRM Institute of Science and Technology, Kattankulathur 603 203, Tamil Nadu, India

et al. 2020; Liu et al. 2020). Over the last several decades, numerous scientific studies have been conducted all over the world in the field of carbon nanomaterials due to their unique (electronic, optical, mechanical, chemical and thermal) properties (Asha and Narain 2020). Carbon materials are, as a rule, biocompatible and contain no resins or other non-organic fillers potentially dangerous for biological objects. One of the varieties of the carbon material graphite is thermally expanded graphite (TEG).

TEG is characterized by a significant electrical conductivity, which is due to its high specific surface area. The process of producing TEG includes three main stages. The first stage is reduced to the introduction of sulfuric or nitric acid molecules in the presence of a strong oxidizer between the layers of the graphite crystal lattice, intercalation. The intercalated graphite compounds are hydrolyzed with water and are then dried to a friable state (Goudarzi and Hashemi Motlagh 2019). After this stage is completed, oxidized graphite is subjected to thermal shock, a high-speed heating up to 800–900 °C. Thermal expansion of intercalated graphite is most effective when exposed to microwave irradiation. Due to the high speed of bulk heating, intercalates' gaseous decomposition products are rapidly released, and graphite particles split practically to graphene layers under the influence of temperature. As a result of volumetric expansion, the interlayer distance of the graphite crystal lattice sharply increases; herewith, the specific surface area of the material increases by an order of magnitude. The degree of expansion of intercalated graphite can be regulated at the stage of hydrolysis. Depending on the presence of intercalate residues, the process of thermal expansion can be continued until the layered structure is completely broken down; herewith, the mechanical properties of the material significantly deteriorate (Chernysheva et al. 2020).

TEG is used as a sorbent for the elimination of emergency oil spills (Tryba et al. 2003), as well as in the production of sheet graphite as a sealer in the metallurgical, chemical, automotive and energy industries (Tyupina et al. 2016). TEG-based composites are used to manufacture electrically conductive items (heaters, electrodes), heat exchangers, gaskets and for other purposes (Afanasov et al. 2009; Li et al. 2007). TEG is also used in bioelectrochemical devices, in particular, in combination with microbial cells and their fragments. Using the thermal expansion of graphite foil, investigators (Chen et al. 2019) succeeded in fabricating effective 3D bioanodes for microbial fuel cells based on *Shewanella oneidensis* MR-1 with a capacity of up to 228 mW m^{-2}. The use of thermally expanded graphite in biosensors made it possible to carry out the mediator-free oxidation of ethanol with membrane fractions of *Gluconobacter oxydans* (Reshetilov et al. 2015). *Gluconobacter* bacteria are often used for the development of electrodes for biosensors and microbial fuel cells (Bertokova et al. 2015). Most of the dehydrogenases, which catalyze the oxidation of a number of lower alcohols and monosaccharides, in *Gluconobacter oxydans* cells are contained not in the cytoplasm, but in the cell membrane (Mientus et al. 2017). Therefore, membrane fractions of *G. oxydans* can be used as an alternative biocatalyst to whole bacterial cells. The addition of a conductive polymer poly(3,4-ethylenedioxythiophene):poly(styrenesulfate) (PEDOT:PSS) enables registering the direct oxidation of glucose by this biocatalyst (Kitova et al. 2021). The enzyme complexes in membrane fractions are surrounded by lipid residues of cell membrane, which protects them from negative external factors. Thus, receptors based on membrane fractions can be more cost-effective compared to enzyme receptors, because they do not require additional procedures of extraction and purification.

The aim of this work was to study the basic bioelectrochemical characteristics of electrodes modified with extra-oxidized TEG. As a rule, TEG obtained by standard methods is characterized by a high degree of chaotic arrangement of layers and possible residues of intercalated particles in the structure. Additional oxidation should result in a greater ordering of the layers in the TEG structure and in the stratification of the material into smaller structures. This process should lead to an increase in the effective surface of the material and an improvement in electrical conductivity, which in general would enable improving the electrochemical parameters of the developed biosensors and MFC.

Material and methods

Membrane fractions of the bacteria *Gluconobacter oxydans* sbsp. *industrius* VKM-1280 were used. The cultivation of the microorganisms is described in Reshetilov et al. (2017). The *G. oxydans* membrane fractions were obtained by ultrasonic dispersion followed by stepwise centrifugation as described in Indzhgiya et al. (2012).

The synthesis of TEG was carried out using the hydrosulfate procedure (Gorshenev et al. 2003). The process included three main stages:

1. Formation of an intercalation compound (graphite hydrosulfate) during the mixing of low-ash graphite for 30 min with a mixture of concentrated nitric and sulfuric acids. The synthesis of graphites modified by acids was carried out in a mixture of concentrated sulfuric and nitric acids at various ratios from 10:1 to 3:1. When modifying graphite particles by a mixture of sulfuric and nitric acids, the intercalation process takes place with the introduction of molecules of the acids into the interlayer space of graphite particles.

2. Removal of acid residues by hydrolysis of graphite intercalation compounds with water and subsequent drying of oxidized graphite to a friable state.
3. Thermal expansion of oxidized graphite at a thermal shock of 800–900 °C to produce TEG. During the heating of modified graphite powder, the lamellar structure of graphite breaks down to be changed by the layered fibrous structure of expanded graphite.

The resulting TEG had a bulk density of $Q_{bulk} = 16$ g/l. Elemental analysis showed TEG to contain up to 0.5 wt % of sulfur as an impurity. Scanning electron microscopy with a resolution of up to 100 nm showed a pronounced lamellar structure of graphite material.

Modified TEG (hereinafter referred to as TEG_M) was obtained by changing the degree of expansion of the original material by an additional thermal treatment by microwave irradiation.

The biosensor was formed using three-contact matrix electrodes (KolorElectronics, Moscow, Russia). A layer of thermally expanded graphite 0.1 mm thick was formed on a working graphite electrode with a diameter of 3 mm by pressing at 150 bar. *G. oxydans* membrane fractions were immobilized on the surface of the working electrode using a conductive gel of poly(3,4-ethylenedioxythiophene):poly(styrenesulfate) (PEDOT:PSS) modified with 3% poly(ethylene glycol) diglycidyl ether (PEGDE). The concentration of membrane fractions on the electrode surface was 0.4 mg/mm^2.

Electrochemical measurements were performed using IPCmicro (KRONAS, Russia) at room temperature and constant stirring in a 25 mM phosphate buffer, pH 6.5, containing 10 mM sodium chloride. Cyclic voltammograms (CV) were recorded in the presence of 42 μM of 2,6-dichlorophenolindophenol (DCPIP) within the range of applied voltages from – 1.0 to 0.5 V at various scan rates. Impedance measurements were performed in a phosphate buffer containing 5 mM of potassium ferrocyanide(III) in the frequency range from 40 kHz to 0.02 Hz at a modulation amplitude of 10 mV (applied potential of 200 mV) using VersaSTAT 4 (Ametek, USA).

The structure of TEG_M was studied using Raman spectroscopy and scanning electron microscopy (SEM). The spectra were taken on a HEDA confocal Raman spectrograph (NOST, South Korea) using a 532 nm laser. SEM images were taken using a Neon 40 Esb-35-09 scanning electron microscope (Carl Zeiss, Germany).

Results and discussion

The structure of thermally expanded graphite

The Raman spectra of the original and modified TEG are shown in Fig. 1A. It is seen that the initial TEG sample at a wavelength of ~ 1581 cm^{-1} has a characteristic "graphite" G peak of high intensity, which corresponds to sp^2 hybridization C in the plane of the graphite grid and is a marker of the sp^2 carbon structure. The peak at a wavelength of ~ 1355 cm^{-1} is a D peak that characterizes the formation of disordered sp^2 hexahedral aromatic rings in the carbon structure. This band is forbidden in ideal graphite and emerges when defects appear in the plane of the carbon network (armchair-type breaks of the carbon rings). The 2D peak is a second-order band—an overtone of the D band at a wavelength of about 2700 cm^{-1}—and shows the "graphene-like" nature of the sample: the higher it is, the more single layered the graphene regions are. Thus, the peak in TEG_M at a wavelength of 1300 cm^{-1} disappears, and the intensity of the peak at a wavelength of 2700 cm^{-1} sharply increases. A decrease in the intensity of the D peak (I_D) compared to the intensity of the G peak (I_G) can be interpreted as the oxidation of a part of the amorphous carbon responsible for the D peak during an "additional expansion" of TEG (Chen et al. 2019). The ratio of the I_D/I_G peaks can be interpreted as an estimate of the degree of disorder in the sp^2-carbon structure (Ferrari 2007). Thus, for the initial TEG the I_D/I_G ratio was 0.61, and for TEG_M it was 0.036. These data show that the TEG sample was stratified into smaller structures and, at the same time, its ordering increased, which may affect its conducting properties.

Figure 1B shows micrographs obtained using scanning electron microscopy. The additional expansion of initial TEG leads to an increase in the distance between the individual graphite layers and to the formation of additional cavities into which bacterial cells can be immobilized.

The conductivity of the obtained samples was assessed by electrochemical impedance spectroscopy. The samples were fixed on the surface of a graphite screen-printed electrode, then the impedance spectra of this system were studied in the presence of potassium hexacyanoferrate(III). The produced Nyquist diagrams are shown in Fig. 2. The impedance spectra were processed using a standard equivalent Randles circuit, in which R_s is the resistance of the solution, R_{CT} is the charge transfer resistance, and C is the capacitance of the double electric layer of the electrode. The values of the parameters of the electrodes with TEG and TEG_M are shown in Table 1.

Thus, additional oxidation of thermally expanded graphite leads to an improvement in the conductive

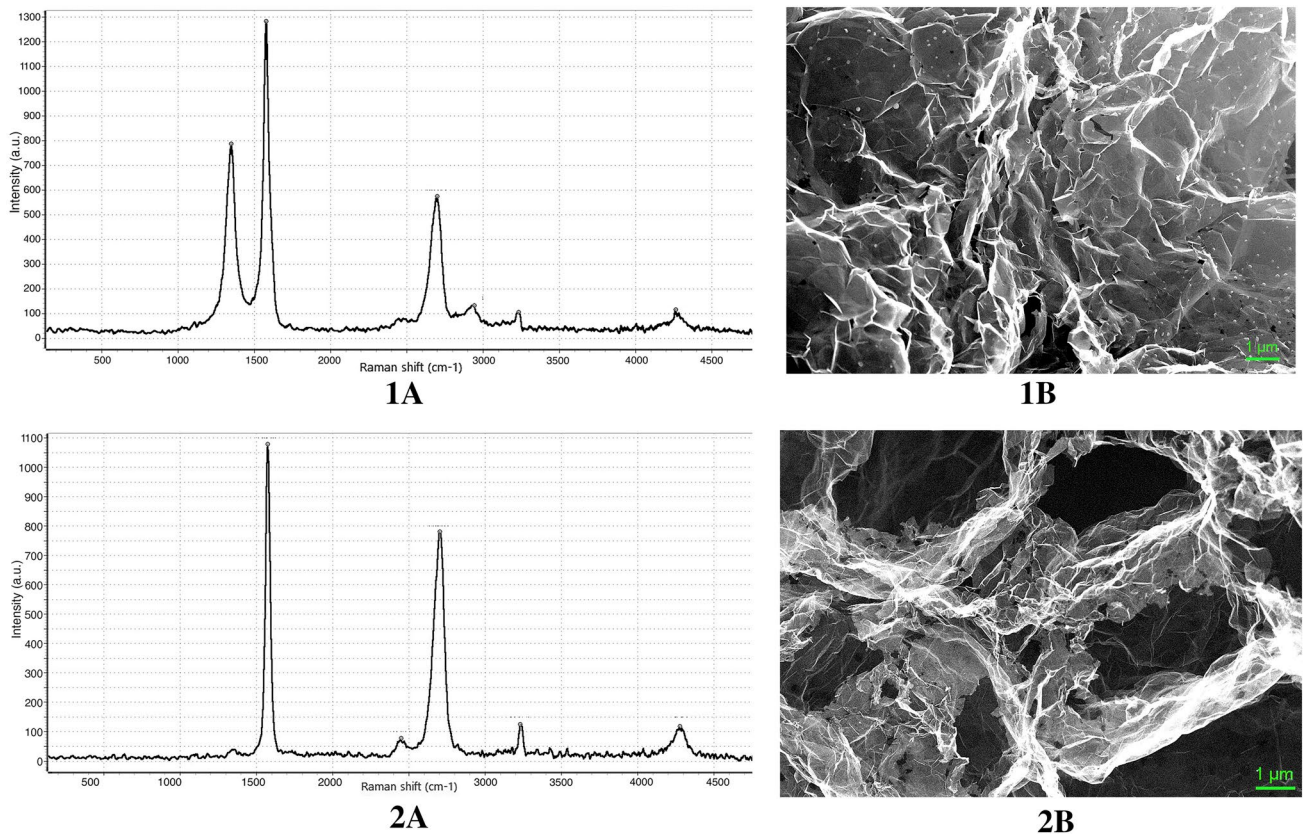

Fig. 1 Raman spectra (**A**) and scanning electron micrographs (**B**) of TEG (1) and TEG_M (2) samples

properties—the charge transfer resistance for the electrode with TEG_M was four times less than for the electrode with the initial TEG. The observed changes are apparently,

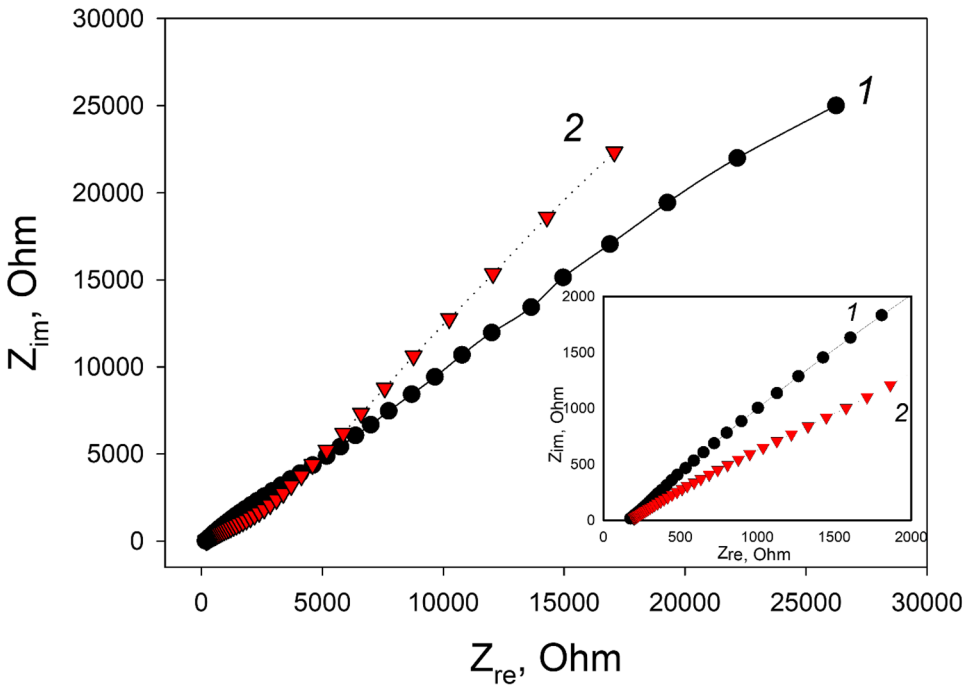

Fig. 2 Nyquist diagrams for electrodes modified with TEG (1) and TEG_M (2). Inset represents the impedance spectra expanded in the high-frequency ranges

Table 1 Parameter values of electrodes with TEG and TEG_M

Electrode	TEG	TEG_M
R_S, ohm	161	179
C, F	7.6×10^{-5}	4.3×10^{-4}
R_{CT}, ohm	1.9×10^{5}	4.7×10^{4}
K_M, mM	2.27 ± 0.17	2.43 ± 0.14
h	2.84 ± 0.46	7.21 ± 1.83
I_{max}, μA	0.79 ± 0.04	0.90 ± 0.03
Linear regression equation	$y = 0.25x - 0.18$	$y = 0.58x - 0.86$
Linear range of detection, mM	1.0–3.0	1.7–3.0
Sensitivity, $\mu A \times mM^{-1} \times cm^{-2}$	3.57	8.28

related to the emergence of a more ordered structure of the nanomaterial.

Calculation of electron charge transfer constants

The reduced charge transfer resistance and high ordering of TEG_M layers make this material promising for use in bioelectrochemical devices. To assess the efficiency of its use, we studied the electrochemical behavior of fragments of microbial cells immobilized on two types of TEG fixed on the surface of graphite screen-printed electrodes. Frequently, bioelectrochemical devices based on microbial cells and their fragments make use of additional compounds (redox mediators) that carry out electron transfer from the active centers of enzymes to the electrode surface. This work used 2,6-dichlorophenolindophenol as a mediator; it is applied in combination with acetic acid bacteria *G. oxydans* (Plekhanova et al. 2018). In the cells–mediator–electrode system, electron transfer proceeds in several stages: diffusion of the mediator to the electrode surface, adsorption of the mediator on the electrode, electron transfer to the electrode, desorption of the reaction product and its diffusion (Bard and Faulkner 2001). The rate of the process is determined by the slowest stage. To identify this stage, as well as to calculate the kinetic constants of electron transfer, we used cyclic voltammetry. The produced cyclic voltammograms of the bioelectrodes based on TEG and TEG_M at different potential scan rates are shown in Fig. 3A. The potential difference between the anode and cathode peaks at the scan rates within the range of 10–110 mV/s for both systems was higher than 59 mV, which is one of the main indicators of a quasi-invertible system (Kasa and Solomon 2016). Another evidence in favor of the assertion that the system is quasi-reversible is the fact that the obtained voltammetry is not symmetrical: the oxidation peak of 2,6-DCPIP in the positive region of applied potentials is in all cases slightly higher than the reduction peak of 2,6-DCPIP in the negative region. Both the cathode and anode peak potentials shifted in the positive and negative directions as the scan rates increased. At the same time, the levels of the redox pair currents increased gradually with an increase in the scan rate. Figure 3B shows linear dependences of the anode and cathode currents on the scan rates for two variants of TEG. The correlation coefficients for all dependences were 0.98–0.99. The linear dependence confirms that the processes occurring on the electrodes are quasi-reversible, and the limiting stage is the transfer of an electron from a biological component on the electrode surface, not the diffusion of the analyte from the solution to the active centers of the enzyme. This coincides with the data obtained by EIS (Fig. 2), where the Nyquist diagrams have no bending of the spectrum at an angle of 45° in the low-frequency region characteristic of systems with diffusion constraints.

Figure 3C shows the dependences of the changes in the cathode and anode peak potentials on the natural logarithm of the scan rate. In the range of scan rates of 0.01–0.11 V/s, the potentials of both the anode and cathode peaks linearly depended on ln υ and the regression equations are shown in the figure. According to the Laviron equation (Laviron 1979):

$$E_p = E^o - \frac{RT}{\alpha n F} \ln \upsilon, \quad (1)$$

where E_p is the anode peak potential; E^0, the standard electrode potential; υ, the scan rate; n, the number of electrons; α, the charge transfer coefficient; R, the gas constant; T, temperature; F, the Faraday constant.

The value of the product $\alpha \times n$ can be calculated from the angle of inclination of the dependences (Elewi et al. 2020) presented in the linear regression equations in Fig. 3C. The value of n was assumed to be equal to two, because two electrons participate in the 2,6-DCPIP redox reaction (Melin and Lohmeier-Vogel 2004). Thus, the value of α for the anode processes was 0.143 for the electrode modified by the initial TEG and 0.165 for the electrode modified by TEG_M.

To estimate the rate of heterogeneous electron transfer, the value of the constant k_s was calculated using the Laviron equation:

$$\ln k_s = \alpha \ln(1-\alpha) + (1-\alpha)\ln\alpha - \ln\frac{RT}{nF\upsilon} - \alpha(1-\alpha)\frac{nF\Delta E_p}{RT}. \quad (2)$$

The value of k_s for the electrode modified by the initial TEG was 0.0296 s^{-1}, and for TEG_M-modified electrode, 0.0350 s^{-1}. Thus, the heterogeneous transfer constant increased by 18%, which is indicative of an acceleration of the electrochemical reaction when using TEG_M.

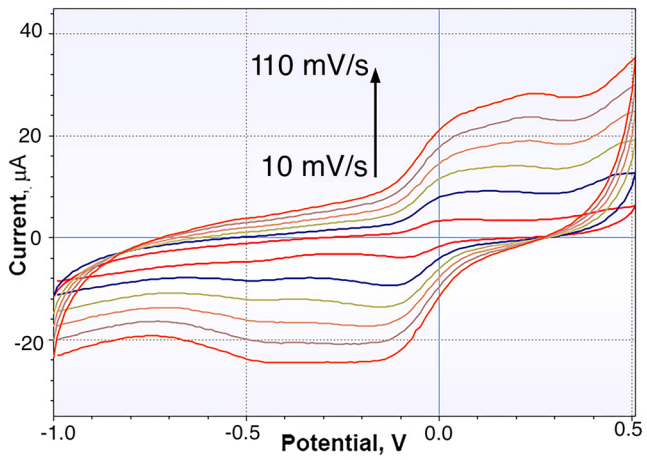

1A

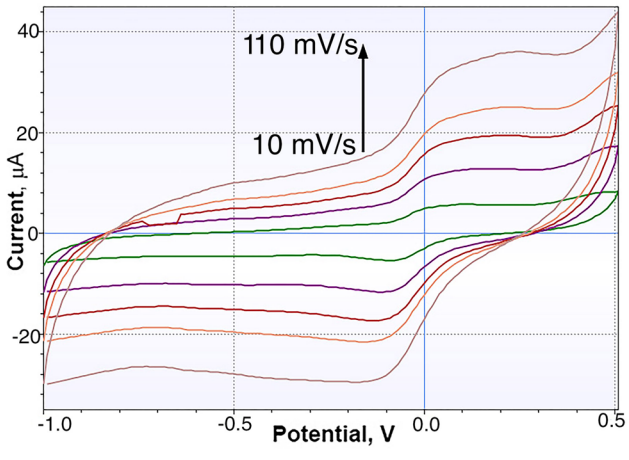

2A

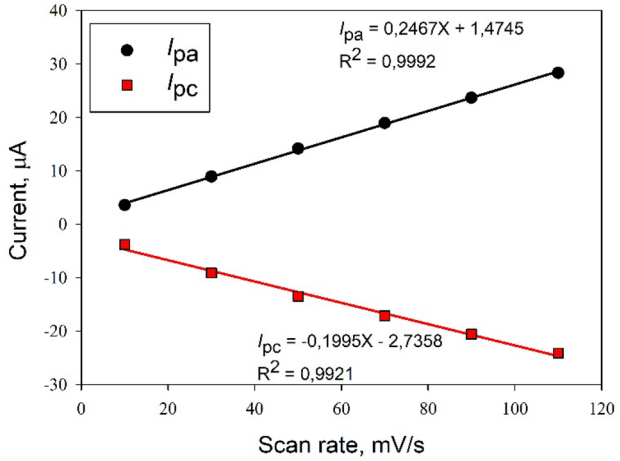

1B

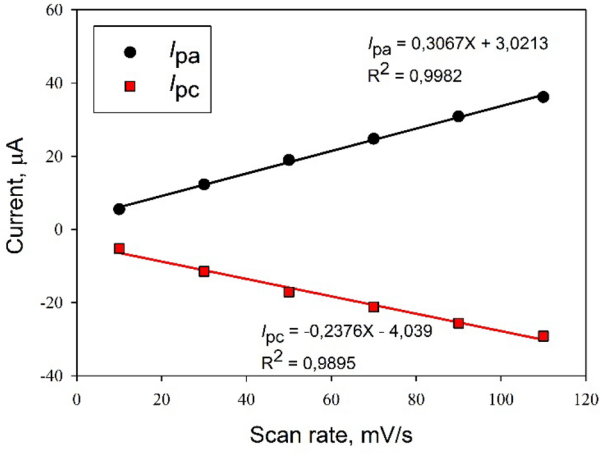

2B

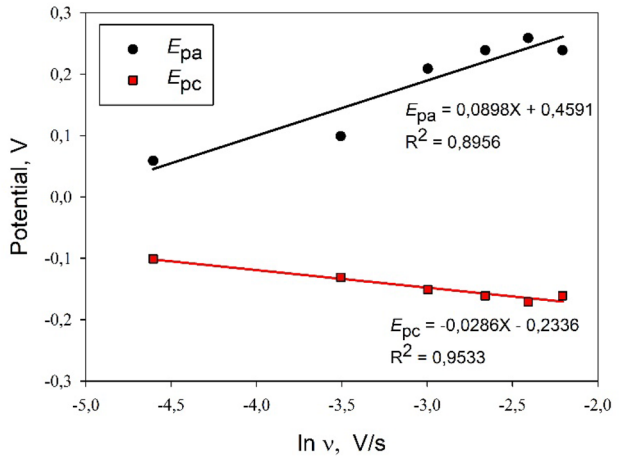

1C

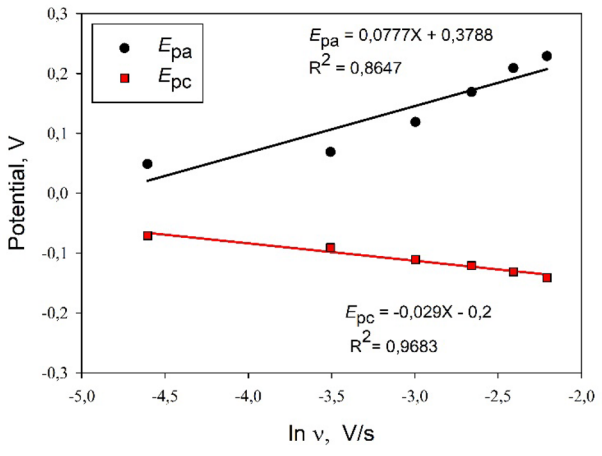

2C

Fig. 3 Electrochemical characteristics of the electrodes modified by TEG (1) and TEG_M (2). **A** Cyclic voltammograms of the electrodes at different scan rates. **B** Linear dependences of the anode and cathode peak currents on the scan rate (I_{pa}, the value of the anode peak; I_{pc}, the value of the cathode peak). **C** Linear dependences of the anode and cathode peak potentials on the natural logarithm of the scan rate (E_{pa}, the potential of the anode peak; E_{pc}, the potential of the cathode peak). Measurements were carried out in the presence of 42 µM DCPIP; scan rates 10–110 mV/s

Calibration curves of biosensors

It was of interest to test the effect of TEG modification on the ability of bioelectrodes formed on its basis to directly transfer charge from biological objects to the electrode, which can be used in the development of third-generation biosensors. For this purpose, *G. oxydans* membrane fractions that make part of the PEDOT conducting gel:PSS–PEGDE were immobilized on the surface of graphite electrodes with TEG and TEG_M. PEDOT:PSS have a mixed electron–ion type of conductivity (Savva et al. 2018). Electron transfer in PEDOT:PSS chains is carried out by a system of conjugated bonds due to electron exchange reactions between neighboring redox sites and is accompanied by conjugated movement of dopants along the polymer chain (Gueye et al. 2019). Pyrroloquinoline quinone (PQQ)-dependent glucose dehydrogenase present in the membrane fractions transfers the electrons produced by glucose oxidation to the electrode modified with TEG without the presence of any additional reagents (Kitova et al. 2021). Most likely, PQQ, which is already present in the membrane fractions of bacteria (Schubart et al. 2012), acts as an electron carrier in this case. It was necessary to determine the effect of additional oxidation of TEG on the possibility of mediatorless electron transfer from membrane fractions. Figure 4A shows the calibration curves of the obtained biosensors.

The detection range of both TEG biosensors was 0.75–10 mM of glucose. The calibration curves were fit by the four-parameter Hill equation:

$$I = I_0 + \frac{I_{\max} \times S^h}{K_M^h + S^h}, \quad (3)$$

where I_{max} is the maximal reaction rate; K_M is the Michaelis constant; h is the cooperativity criterion.

The values of the biosensors' parameters are presented in Table 1.

As can be seen from the presented data, the modification of TEG leads to a significant increase in the sensitivity of the biosensor to glucose (from 3.57 to 8.28 $\mu A \times mM^{-1} \times cm^{-2}$), as well as to an increase of the Hill coefficient from 2.84 to 7.21. The Hill coefficient (h) is a dimensionless value that characterizes the cooperativity of ligand binding by the enzyme. As can be seen from the data obtained, in both cases the value of h is greater than unity, i.e., a positive cooperativity of the enzymes is observed for the immobilized membrane fractions; the cooperativity increases significantly when TEG is replaced by its modified version.

We obtained the calibration curves for the main substrates of the membrane fractions of *G. oxydans* in a composite with PEDOT:PSS and TEG_M when using the electronic transport mediator 2,6-DCPIP. The addition of redox mediators allows the system to produce higher currents which leads to the increase of the efficiency of bioelectrochemical devices and to the expansion of its practical application. This composite can be used both in second-generation biosensors and in biofuel-cell bioanodes. The obtained calibration curves are shown in Fig. 4B; the parameter values for these dependences are in Table 2.

G. oxydans are widely used in biotechnological processes to obtain acetic acid from alcohols, which indicates

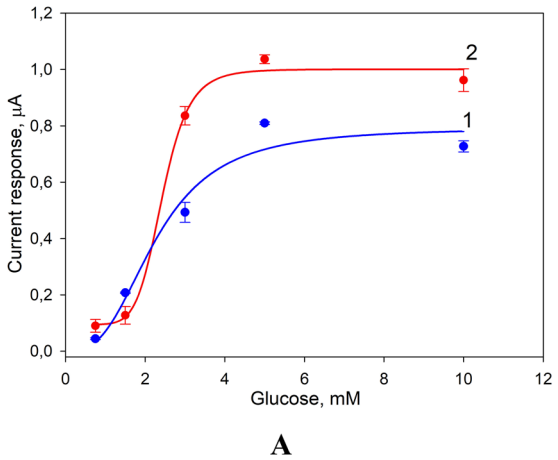

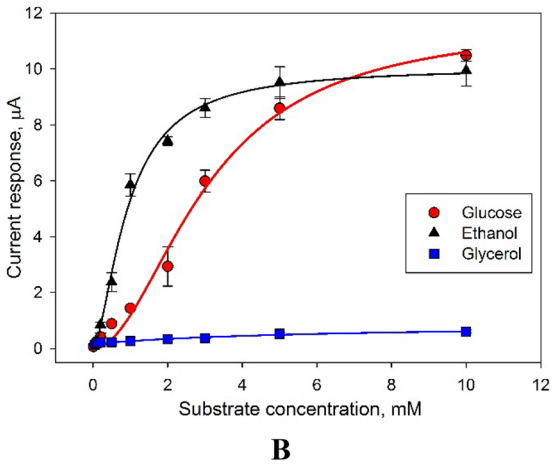

Fig. 4 **A** Calibration curves for glucose biosensors based on electrodes modified by TEG (1) and TEG_M (2). *G. oxydans* membrane fractions were used as a biocatalyst. The data in the absence of redox mediators are presented. Measurements were carried out at an applied potential of + 400 mV vs. Ag/AgCl electrode. **B** Calibration curves for a biosensor based on *G. oxydans* membrane fractions and an electrode modified with TEG_M for three analytes. The data in the presence of the redox mediator 2,6-DCPIP (42 μM) are given. Measurements were carried out at an applied potential of + 200 mV vs. Ag/AgCl electrode

Table 2 Parameter values of biosensors with TEG_M for various analytes

Analyte	Glucose	Glycerol	Ethanol
Parameter			
K_M, mM	3.05	0.16	0.93
h	1.95	0.97	1.6
I_{max}, μA	11.65	0.74	10.06
Linear regression equation	$y = 2.12x–0.79$	$y = 0.05x + 0.24$	$y = 5.48x–0.13$
Linear range of detection, mM	0.5–4.0	1.0–6.0	0.1–1.2
Sensitivity, $\mu A \times mM^{-1} \times cm^{-2}$	30.28	0.71	78.29

the high activity of alcohol dehydrogenases of these cells (Gupta et al. 2001). The developed biosensor demonstrates the greatest sensitivity in ethanol measurements (78.29 $\mu A \times mM^{-1} \times cm^{-2}$). The sensitivity to glucose is lower (30.28 $\mu A \times mM^{-1} \times cm^{-2}$), but it still remains at a fairly high level. The lowest biosensor sensitivity was observed for glycerol, which is explained by the fact that glycerol has an inhibitory effect, and its oxidation product (dihydroxyacetone) can damage *Gluconobacter* cells (Ohrem and Voss 1996).

Acetic acid bacteria *G. oxydans* differ in the membrane localization of the main enzyme complexes, which facilitates their interaction with electron transport mediators. Therefore, the use of membrane fractions of these bacteria enables producing a fairly universal biocatalyst capable of oxidizing a wide range of compounds. This property can be useful not only in biosensors, but also for creation of MFCs. These MFC can be used for purifying the effluents of fermentation plants, related to the food or alcohol industry, because the effluents may contain residual sugars and alcohols, as well as other organic compounds that pollute the environment.

Conclusions

The paper considered features of the properties of thermally expanded graphite with different degrees of expansion. Using Raman spectroscopy, the study showed that modified TEG was stratified into smaller structures compared with the original TEG; herewith, the ordering of the layers and the similitude of the material to graphene increased. The ratio of I_D/I_G peak intensities for the initial TEG was 0.61; for TEG_M, 0.036. The effective surface of the material, capable of adsorbing bacterial cells, also increased. With the used way of enhancing screen-printed graphite electrodes with modified TEG, the electrode charge transfer resistance was decreased fourfold as compared with the original TEG. Based on TEG-modified screen-printed electrodes, biosensors with *G. oxydans* membrane fractions were constructed. The constants of heterogeneous charge transfer in the membrane fractions–DCPIP–electrode system at the modification of the electrode by two variants of TEG were assessed. The heterogeneous transfer rate constant for an electrode with TEG_M increased by 18% compared with the initial variant, which is indicative of an acceleration of the electrochemical reaction when using TEG_M. The possibility of creating third-generation mediator-free biosensors for glucose detection was shown. The use of TEG_M instead of TEG in this biosensor made it possible to increase the sensitivity of the biosensor to glucose twofold. The possibility of using these bioelectrodes in second-generation mediator biosensors for the determination of glucose, ethanol and glycerol was assessed. This biosensor demonstrated the highest sensitivity in ethanol measurements (78.29 $\mu A \times mM^{-1} \times cm^{-2}$).

Thus, the membrane fractions–TEG_M composite can be used to develop second- and third-generation biosensors, as well as in MFC, which can be utilized in fermentation plants, performing a dual function of electricity generation from glucose and ethanol present in the distillery stillage, and purification of alcohol-production effluents.

Acknowledgements The reported study was funded by RFBR and DST according to the research project No. 19-58-45011 (section of bioelectrochemical measurements). The reported study was also funded by RFBR according to the research project No. 18-29-23042 (section of spectral measurements). The authors are grateful to Aleksandr Bykov for the cultivation of bacterial cells and production of bacterial membrane fractions. Victor Selivanov is acknowledged for linguistic help.

Declarations

Conflict of interest The authors declare that they have no conflict of interest in the publication.

References

Afanasov IM, Morozov VA, Kepman AV, Ionov SG, Seleznev AN, Tendeloo GV, Avdeev VV (2009) Preparation, electrical and thermal properties of new exfoliated graphite-based composites. Carbon 47(1):263–270. https://doi.org/10.1016/j.carbon.2008.10.004

Asha AB, Narain R (2020) Nanomaterials properties. In: Narain R (ed) Polymer science and nanotechnology. Fundamentals and applications. Elsevier Inc., Amsterdam, pp 343–359. https://doi.org/10.1016/b978-0-12-816806-6.00015-7

Bard AJ, Faulkner LR (2001) Electrochemical methods. Fundamentals and applications, vol 2. Wiley, New York

Berillo D, Al-Jwaid A, Caplin J (2021) Polymeric materials used for immobilisation of bacteria for the bioremediation of contaminants in water. Polymers 13:1073. https://doi.org/10.3390/polym13071073

Bertokova A, Bertok T, Filip J, Tkac J (2015) *Gluconobacter* sp. cells for manufacturing of effective electrochemical biosensors and biofuel cells. Chem Pap 69(1):28–41. https://doi.org/10.1515/chempap-2015-0040

Chen L, Li Y, Yao J, Wu G, Yang B, Lei L, Hou Y, Li Z (2019) Fast expansion of graphite into superior three-dimensional anode for microbial fuel cells. J Power Sources 412:86–92. https://doi.org/10.1016/j.jpowsour.2018.11.033

Chernysheva MN, Rychagov AY, Kornilov DY, Tkachev SV, Gubin SP (2020) Investigation of sulfuric acid intercalation into thermally expanded graphite in order to optimize the synthesis of electrochemical graphene oxide. J Electroanal Chem 858:113774. https://doi.org/10.1016/j.jelechem.2019.113774

Do MH, Ngo HH, Guo W, Chang SW, Nguyen DD, Liu Y et al (2019) Microbial fuel cell-based biosensor for online monitoring wastewater quality: a critical review. Sci Total Environ 712:135612. https://doi.org/10.1016/j.scitotenv.2019.135612

Elewi AS, Al-Shammaree SAW, Al-Sammarraie AKMA (2020) Hydrogen peroxide biosensor based on hemoglobin-modified gold nanoparticles–screen printed carbon electrode. Sens Bio-Sens Res. https://doi.org/10.1016/j.sbsr.2020.100340

Ferrari AC (2007) Raman spectroscopy of graphene and graphite: disorder, electron–phonon coupling, doping and nonadiabatic effects. Solid State Commun 143(1–2):47–57. https://doi.org/10.1016/j.ssc.2007.03.052

Gorshenev VN, Bibikov SB, Novikov YN (2003) Conducting materials based on thermally expanded graphite. Russ J Appl Chem 76(4):603–606

Goudarzi R, Hashemi Motlagh G (2019) The effect of graphite intercalated compound particle size and exfoliation temperature on porosity and macromolecular diffusion in expanded graphite. Heliyon 5(10):e02595. https://doi.org/10.1016/j.helyon.2019.e02595

Gueye MN, Carella A, Faure-Vincent J, Demadrille R, Simonato J-P (2019) Progress in understanding structure and transport properties of PEDOT-based materials: a critical review. Prog Mater Sci 108:100616. https://doi.org/10.1016/j.pmatsci.2019.100616

Guo Y, Wang J, Shinde S et al (2020) Simultaneous wastewater treatment and energy harvesting in microbial fuel cells: an update on the biocatalysts. RSC Adv 10(43):25874–25887. https://doi.org/10.1039/d0ra05234e

Gupta A, Singh VK, Qazi G, Kumar A (2001) *Gluconobacter oxydans*: Its biotechnological applications. J Mol Microbiol Biotechnol 3:445–456

Hwang HS, Jeong JW, Kim YA, Chang M (2020) Carbon nanomaterials as versatile platforms for biosensing applications. Micromachines 11:814. https://doi.org/10.3390/mi11090814

Indzhgiya EY, Ponamoreva ON, Alferov VA, Reshetilov AN, Gorton L (2012) Interaction of ferrocene mediators with *Gluconobacter oxydans* immobilized whole cells and membrane fractions in oxidation of ethanol. Electroanalysis 24(4):924–930. https://doi.org/10.1002/elan.201100425

Kasa T, Solomon T (2016) Cyclic voltammetric and electrochemical simulation studies on the electro-oxidation of catechol in the presence of 4,4-bipyridine. Am J Phys Chem 5(3):45–55. https://doi.org/10.11648/j.ajpc.20160503.11

Kitova A, Tarasov S, Plekhanova Y, Bykov A, Reshetilov A (2021) Direct bioelectrocatalytic oxidation of glucose by *Gluconobacter oxydans* membrane fractions in PEDOT:PSS/TEG-modified biosensors. Biosensors 11:144. https://doi.org/10.3390/bios11050144

Laviron E (1979) General expression of the linear potential sweep voltammogram in the case of diffusionless electrochemical systems. J Electroanal Chem Interf Electrochem 101(1):19–28. https://doi.org/10.1016/s0022-0728(79)80075-3

Li W, Han C, Liu W, Zhang M, Tao K (2007) Expanded graphite applied in the catalytic process as a catalyst support. Catal Today 125(3–4):278–281

Li M, Li Y-W, Cai Q-Y, Zhou S-Q, Mo C-H (2020) Spraying carbon powder derived from Mango Wood biomass as High-performance Anode in Bio-electrochemical system. Biores Technol 300:122623. https://doi.org/10.1016/j.biortech.2019.122623

Liu Y, Zhang X, Zhang Q, Li C (2020) Microbial fuel cells: nanomaterials based on anode and their application. Energy Technol 8(9):2000206. https://doi.org/10.1002/ente.202000206

Melin AD, Lohmeier-Vogel EM (2004) Using cytochome *c* to monitor electron transport and inhibition in beef heart submitochondrial particles. Biochem Mol Biol Educ 32(1):39–44. https://doi.org/10.1002/bmb.2004.494032010306

Mientus M, Kostner D, Peters B, Liebl W, Ehrenreich A (2017) Characterization of membrane-bound dehydrogenases of *Gluconobacter oxydans* 621H using a new system for their functional expression. Appl Microbiol Biotechnol 101(8):3189–3200. https://doi.org/10.1007/s00253-016-8069-4

Ohrem HL, Voss H (1996) Inhibitory effect of glycerol on *Gluconobacter oxydans*. Biotechnol Lett 18:245–250

Plekhanova Y, Tarasov S, Kolesov V, Kuznetsova I, Signore M, Quaranta F, Reshetilov A (2018) Effects of polymer matrices and carbon nanotubes on the generation of electric energy in a microbial fuel cell. Membranes 8:99. https://doi.org/10.3390/membranes8040099

Reshetilov AN, Kitova AE, Kolesov VV, Yaropolov AI (2015) Mediator-free bioelectrocatalytic oxidation of ethanol on an electrode from thermally expanded graphite modified by *Gluconobacter oxydans* membrane fractions. Electroanalysis 27:1443. https://doi.org/10.1002/elan.201400610

Reshetilov AN, Plekhanova YV, Tarasov SE, Arlyapov VA, Kolesov VV, Gutorov MA, Gotovtsev PM, Vasilov RG (2017) Effect of some carbon nanomaterials on ethanol oxidation by *Gluconobacter oxydans* bacterial cells. Appl Biochem Microbiol 53(1):123–129. https://doi.org/10.1134/s0003683817010161

Savva A, Wustoni S, Inal S (2018) Ionic-to-electronic coupling efficiency in PEDOT:PSS films operated in aqueous electrolytes. J Mat Chem C 6:12023–12030. https://doi.org/10.1039/c8tc02195c

Schubart IW, Göbel G, Lisdat FA (2012) Pyrroloquinolinequinone-dependent glucose dehydrogenase (PQQ-GDH)-electrode with direct electron transfer based on polyaniline modified carbon nanotubes for biofuel cell application. Electrochim Acta 82:224–232

Sun H, Angelidaki I, Wu S, Dong R, Zhang Y (2019) The Potential of bioelectrochemical sensor for monitoring of acetate during anaerobic digestion: focusing on novel reactor design. Front Microbiol 9:3357. https://doi.org/10.3389/fmicb.2018.03357

Tryba B, Morawski AW, Kaleńczuk RJ, Inagaki M (2003) Exfoliated graphite as a new sorbent for removal of engine oils from wastewater. Spill Sci Technol B 8(5–6):569–571. https://doi.org/10.1016/s1353-2561(03)00070-7

Tyupina EA, Sazonov AB, Sergeecheva YV, Shestakov IA, Tuchkova AI, Nikitin AV (2016) Application of thermally expanded graphite for the cementation of cesium and tritium containing waste oils. Inorg Mater Appl Res 7(2):196–203